ELSEVIER

Journal of Molecular Catalysis A: Chemical 189 (2002) 233–240

JOURNAL OF MOLECULAR CATALYSIS A: CHEMICAL

www.elsevier.com/locate/molcata

Evaluation of silica-supported zirconocenes in ethylene/1-hexene copolymerization

Griselda B. Galland*, Marcus Seferin, Rafael Guimarães, Juliana A. Rohrmann, Fernanda C. Stedile, João H.Z. dos Santos

Instituto de Química, Universidade Federal do Rio Grande do Sul, Av. Bento Gonçalves 9500, 91509-900 Porto Alegre, RS, Brazil

Received 31 January 2002; received in revised form 25 February 2002; accepted 3 April 2002

Abstract

A series of zirconocenes differing in the coordination sphere, namely (R)$ZrCl_2$ (R = $(MeCp)_2$, $(i\text{-}BuCp)_2$, $(n\text{-}BuCp)_2$, *rac*-$Et(Ind)_2$ and *rac*-$Et(IndH_4)_2$) were immobilized on silica Grace 948 pretreated at 723 K under vacuum. The highest metal loading, determined by Rutherford's backscattering spectrometry (RBS) and X-ray photoelectron spectroscopy, was achieved with *rac*-$Et(Ind)_2ZrCl_2$. The steric effect played by the ligands on the cyclopentadienyl ring was seen to influence on the grafted content: less Zr was immobilized on silica using *n*-Bu as ligand, as compared to the zirconocene that uses Me as ligand. Nevertheless, this catalyst was the most active both in homogeneous and supported copolymerizations. Copolymers were characterized with respect to their molecular weights, polydispersity (M_w/M_n), crystallinity, comonomer incorporation and melting temperature.
© 2002 Elsevier Science B.V. All rights reserved.

Keywords: Metallocene; Supported catalysts; Polyethylene; Ethylene/1-hexene copolymers

1. Introduction

A variety of polyolefins is accessible by catalytic polymerization processes ranging from very low up to ultrahigh molecular mass compounds covering a broad range of densities. Polyethylene is a commodity with a great industrial importance (47.8 million tons in 1999) due to the versatility of its physical and chemical properties. Linear low density polyethylene (LLDPE), a copolymer of ethylene and α-olefins, is the polyethylene that presents the highest industrial rate of growth (11.2% per year) and it might substitute some other plastics in the future [1,2].

In the above mentioned process, the catalyst system plays a key role, determining the polymerization behavior, polymer structure and, in heterogeneous processes, polymer powder morphology. Metallocene/methylaluminoxane (MAO) homogeneous catalysts provide olefin polymers with characteristics which are distinguished from those obtained by conventional Ziegler–Natta catalyzed polymers, such as their narrower molecular weight distribution and composition distribution. However, being homogenous catalysts, such systems present disadvantages in regard to their application for industrial use, particularly concerning gas phase processes. One approach to overcome this problem consists of the heterogeneization of such catalysts, by supporting them on carriers. Several routes, employing different supports, are described in the scientific and patent literatures (see, for example [3]).

Silica has been the preferred support for metallocene immobilization. In addition to controlling

* Corresponding author.

1381-1169/02/$ – see front matter © 2002 Elsevier Science B.V. All rights reserved.
PII: S1381-1169(02)00180-2

polymer morphology, silica's unique surface chemistry, namely, the concentration and strength of hydroxyl groups and siloxane bridges, can be used to immobilize reagents. Besides, silica allows a controlled fragmentation during polymerization reaction, thus leading to the formation of uniform polymer particles with a narrow particle size distribution and high bulk density [4].

In general, immobilization methods can be classified in three categories: direct adsorption on the support (see, for example [5]), chemical modification of silica with MAO [6], alkylaluminum [7], organosilanes (see, for example [8]), or borates [9], prior to metallocene grafting, and finally the in situ synthesis of metallocenes on silica [10], on polymer support [11] or even the synthesis of the silica and the metallocene by the sol–gel method [12]. All these procedures afford different catalysts and these in turn produce polyolefins with different properties. In the present study, we chose the direct adsorption, which is believed to afford polymers with higher molecular weight.

In a previous paper [13] we studied the effect of comonomer concentration on catalyst activity, on comonomer incorporation and on polymer properties in ethylene/1-hexene copolymerization using (n-BuCp)$_2$ZrCl$_2$/SiO$_2$ catalyst system. In the present study, we expanded this study to other silica-supported catalyst systems, aiming at studying the steric effect played by the metallocene ligands on final zirconocene loading, on catalyst activity and on comonomer incorporation. Metal content was determined by Rutherford's backscattering spectrometry (RBS), while Zr/Si ratios and the nature of the surface species were probed by X-ray photoelectron spectroscopy (XPS). Supported catalysts were evaluated in terms of ethylene/1-hexene slurry copolymerization catalyst activities as well as from resulting polymer characteristics, namely, molecular weight, polydispersity (M_w/M_n), crystallinity, comonomer incorporation and melting (T_m) temperature.

2. Experimental part

2.1. Materials (chemicals)

Silica Grace 948 (255 m^2 g^{-1}) was activated under vacuum ($P < 10^{-4}$ mbar) for 16 h at 723 K. The support was then cooled to room temperature under dynamic vacuum and stored under dried argon. MAO was gently supplied by Witco (10.0 wt.% toluene solution, 1.7 Al as TMA, average molar mass 900 g mol^{-1}). The metallocenes (n-BuCp)$_2$ZrCl$_2$, (MeCp)$_2$ZrCl$_2$, (i-BuCp)$_2$ZrCl$_2$, rac-Et(Ind)$_2$ZrCl$_2$ and rac-Et(IndH$_4$)$_2$ZrCl$_2$ (all supplied by Witco) were used without further purification. Pure grade toluene and 1-hexene (Aldrich) were deoxygenated and dried by standard techniques. Ethylene, provided by COPESUL Co., and argon were deoxygenated and dried through columns of BTS (gently supplied by BASF) and activated molecular sieves (13 Å) prior to use.

2.2. Preparation of supported catalysts

All grafting experiments were performed under inert atmosphere using the Schlenk technique. Typically, toluene solutions of metallocene were added to 1.5 g of pretreated silica Grace 948, in concentration corresponding to 1.5 wt.% Zr/SiO$_2$ and the suspension stirred for 1 h at 353 K. The slurry was then filtered through a fritted disk. The resulting solids were washed with 12 cm^3 × 2.0 cm^3 of toluene and dried under vacuum for 4 h.

2.3. Catalyst characterization

2.3.1. Rutherford's backscattering spectrometry (RBS)

Zirconium loadings in catalysts were determined by RBS using He$^+$ beams of 2.0 MeV, produced by a 3 MV Tandetron (High Voltage Engineering Europa) accelerator incident on homogeneous tablets of the compressed (12 MPa) powder of the catalyst systems. During analysis the base pressure in the chamber is kept in the 10^{-7} mbar range using membrane (to prevent oil contamination of the sample) and turbo-drag molecular pumps. The method is based on the determination of the number and the energy of the detected particles, which are elastically scattered in the Coulombic field of the atomic nuclei in the target. In this study, the Zr/Si atomic ratio was determined from the heights of the signals corresponding to each of the elements in the spectra and converted to wt.% Zr/SiO$_2$. For an introduction to the method and applications

of this technique the reader is referred elsewhere [14,15].

2.4. X-ray photoelectron spectroscopy (XPS)

X-ray photoelectron spectra were obtained on a PHI 5600 Esca System (Φ Physical Eletronics) using monochromated Al Kα (2 mm) radiation (1486.6 eV). Spectra were taken at room temperature in low resolution (pass energy 235 eV) in the range of 1000–0 eV binding energy (BE) and in high-resolution (pass energy 11.75 with 0.05 eV resolution) modes for the Si 2p, Al 2p and Zr 3d regions.

Samples were mounted on an adhesive copper tape. They were prepared in a glove box, transferred under nitrogen atmosphere and then evacuated until reaching 10^{-6} mbar using a turbomolecular pump in an introduction chamber. During data collection, the ion pumped analysis chamber was maintained at $<5 \times 10^{-9}$ mbar. Take-off angle (angle between the surface plane and the detector) was 75°. Normally 50 scans were signal averaged for selected BE windows and processed by the software supplied by the manufacturer. Current of the electron flood gun (neutralizer) was 21.5 mA.

Binding energies examined (element, transition, and range scanned) were as follows: Si 2p, 96–108 eV; Al 2p, 70–80 eV; and Zr 3d, 176–188 eV. In the case of silica-supported systems, all binding energies values were charge referenced to the silica Si 2p at 103.3 eV. Otherwise, they were referenced to the Au $4f_{7/2}$ peak at 84.0 eV.

Estimation of surface atomic ratios was based on integrated areas and calculated atomic sensitivities factors, which were empirically derived for the electron energy analyzer supplied by Perkin-Elmer: Si 2p: 56.65, Al 2p: 57.59, Zr $3d_{5/2}$: 439.98.

Three measurements per sample were performed, and the reproducibility of the XPS analysis was confirmed. For each of the XPS spectra reported, an attempt has been made to deconvolute the experimental curve in a series of components that represent the contribution of the photoelectron emission from atoms in different chemical environments. Individual lines are described as having Gaussian and Lorentzian contributions in order to take into account the effects of the instrumental error and the line shape characteristic of the photoemission process.

2.5. Polymerization reactions

Ethylene/1-hexene copolymerizations were performed in 0.3 l of toluene in a 1.0 l Pyrex glass reactor connected to a constant temperature circulator, equipped with a mechanical stirring and inlets for argon and the ethylene. MAO was used as co-catalyst in an Al/Zr molar ratio of 2500. For each experiment 2×10^{-6} mol of Zr catalyst was suspended in toluene and transferred into the reactor under argon. The polymerizations were performed at 1.6 bar pressure of ethylene at 60° C for 30 min. The reagents were introduced in the reactor in the following order: toluene, MAO, comonomer, monomer and catalyst. Acidified (HCl) ethanol was used to quench the processes. Reaction products were separated by filtration, washed with distilled water, and finally dried under reduced pressure at room temperature.

2.6. Polymers characterization

Polymer melting points (T_m) and crystallinities (X_c) were determined on a TA 2100 Thermal Analyst differential scanning calorimeter calibrated with Indium, using a heating rate of 10 °C min^{-1} in the temperature range of 30–160° C. The heating cycle was performed twice, but only the results of the second scan are reported.

Molar masses and molar mass distributions were investigated with a Waters high-temperature GPC instrument, CV 150C, equipped with optic differential refractometer and three Styragel HT type columns (HT3, HT4 and HT6) with exclusion limit 10^7 for polystyrene. 1,2,4-Trichlorobenzene was used as solvent, at a flow rate of 1 l min^{-1}. The analyses were performed at 140° C. The columns were calibrated with standard narrow molar mass distribution polystyrenes and then universally with LLDPEs and polypropylenes.

^{13}C-NMR was employed to determine the composition and sequence distribution of the copolymers according to procedures in the literature [16]. The ^{13}C-NMR spectra were recorded at 90 °C using a Varian 300 spectrometer operating at 75 MHz. Sample solutions of the copolymer were prepared in *o*-dichlorobenzene and benzene-d_6 (20 v/v). Spectra were taken with a 74° flip angle, an acquisition time of 1.5 s and a delay of 4.0 s. Under these conditions

the spectra are 90% quantitative if only carbon atoms that have a relaxation time (T_1) inferior to 2.0 s are taken into account [17].

3. Results and discussion

The immobilization of metallocenes on the silica surface takes place by the reaction between silica silanol groups (Si–OH) and the metallocene ligands (in the present case, chlorides). After heat treatment under vacuum at elevated temperatures (>450 °C), silica presents mainly isolated single and, to a lesser extent, geminal hydroxyl groups, as well as surface siloxane bridges [18]. In a previous study, we observed in situ FT-IR spectroscopy that metallocene ligands themselves might exert some steric effect preventing further reaction between them and silanol groups remaining on the surface [19]. In order to have a more complete picture, we decided to study the effect of various metallocene ligands, differing in steric and electronic effect, on the surface metal loading and on catalyst activity. Three classes of compounds were employed: cyclopentadienyl complexes containing alkyl substituent on the Cp ring (methyl, *n*-butyl, *i*-butyl); indenyl metallocene and a hydrogenated indenyl complex.

Table 1 reports the resulting metal loading for the different supported systems prepared under otherwise identical conditions. Metal content was determined by RBS and XPS. Surface area measurements by the BET method before and after Cp_2ZrCl_2 grafting did not show any difference, suggesting that silica pores are neither blocked, neither reduced [5]. In other words, catalyst grafting might take place preferentially at the external surface of the silica grains. According to Table 1, values measured by RBS are systematically lower than those obtained by XPS. In the case of RBS, assuming that silica is in its crystalline form (α-quartz), the penetration of 2.0 MeV He^+ ions in the support would be 8% of silica particle diameter (≅6 μm). On the other hand, XPS sampling depth is roughly 4 nm. Therefore, XPS is more sensitive to the outer surface composition, where the relative concentration of Zr atoms is much more localized. Although, *rac*-Et(Ind)$_2$ZrCl$_2$ has shown the highest grafted-metal content among the catalysts tested, this value was much higher in the case of XPS measurements. It is worth mentioning that error is ca. 10% in the case of RBS, while much lower than 5% in the case of XPS. In spite of the numeric differences between both techniques, grafted-metal content showed the same trend among the different supported catalysts.

Table 1
Zr loading on silica, for different supported metallocene systems, determined by RBS and XPS

Metallocene	Zr/SiO_2 (wt.%)	
	RBS	XPS
$(MeCp)_2ZrCl_2$	1.0	1.4
$(n\text{-}BuCp)_2ZrCl_2$	0.8	1.2
$(i\text{-}BuCp)_2ZrCl_2$	0.8	1.1
Et(Ind)$_2$ZrCl$_2$	1.5	4.7
Et(IndH$_4$)$_2$ZrCl$_2$	0.7	1.1

Comparing substituted cyclopentadienyl metallocenes, the presence of larger groups (*n*-Bu and *i*-Bu) reduces the grafted metallocene content, but between both ligands there is no difference.

The immobilization of *rac*-Et(Ind)$_2$ZrCl$_2$ led to the highest metal content as compared to the preceding systems. Similar metal content values (all of them determined by inductively coupled plasma, ICP) were reported in the literature: the immobilization of *rac*-Et(Ind)$_2$ZrCl$_2$ carried out at 343 K in toluene for 16 h was shown to graft 1.35 wt.% Zr/SiO_2 [20]. Also 1.53 wt.% Zr/SiO_2 were obtained for the same catalyst when grafting was performed for 18 h at 343 K [21]. Kaminsky and Renner [22] found 1.45 wt.% Zr/SiO_2, grafting Et(Ind)$_2$ZrCl$_2$ for 16 h at 343 K, followed by Soxlet extraction with toluene for 2 days. Among the tested metallocenes, *rac*-Et(IndH$_4$)$_2$ZrCl$_2$ led to the lowest metal content. Collins et al. [23] reported 1.47 and 0.67 wt.% Zr/SiO_2 grafted on partially dehydroxylated silica using *rac*-Et(Ind)$_2$ZrCl$_2$ and *rac*-Et(IndH$_4$)$_2$ZrCl$_2$, respectively.

XPS characterization of the catalysts showed two lines, due to spin–orbit coupling, in the Zr 3d spectrum of neat $(MeCp)_2ZrCl_2$ (Fig. 1 (top)): ca. 182.0 ($3d_{5/2}$) and 184.5 eV ($3d_{3/2}$). For the sake of simplicity, in the following discussion we will take into account only the $3d_{5/2}$ lines, despite appearing in the figures the contributions of both $3d_{5/2}$ and $3d_{3/2}$.

After immobilization on silica (Fig. 1 (bottom)), two species (seen as four signals due to spin–orbit

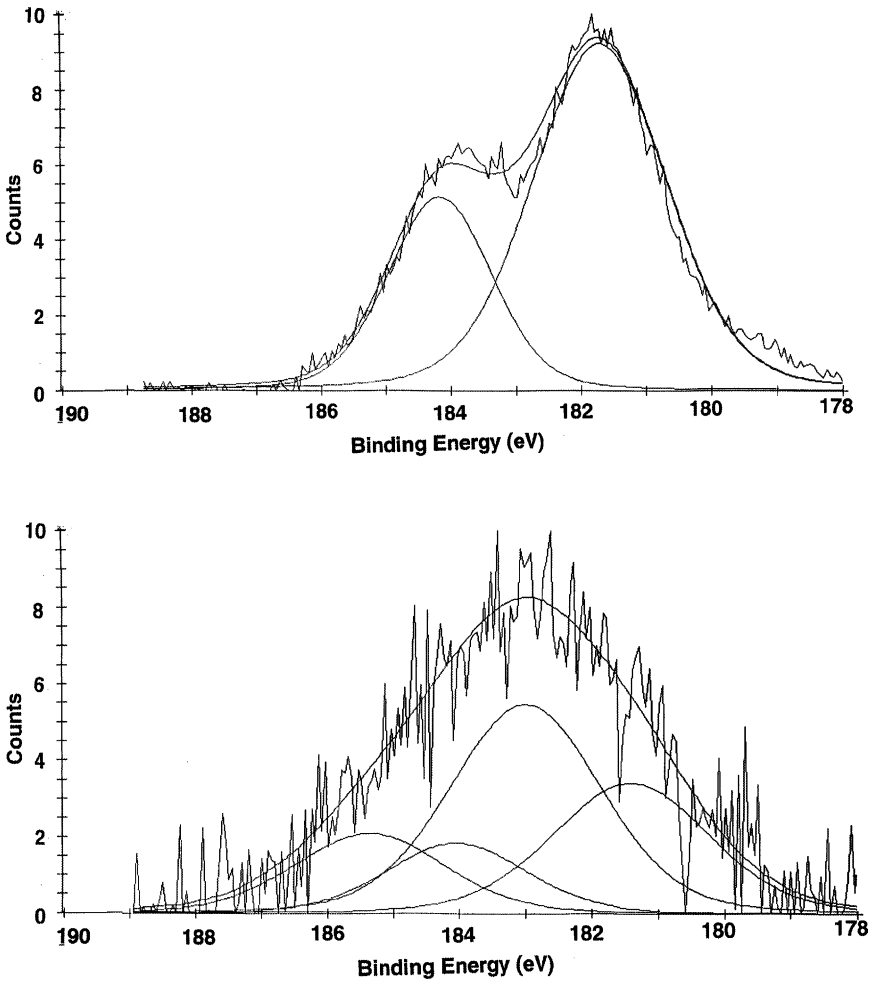

Fig. 1. XPS spectra of Zr 3d core level region of $(MeCp)_2ZrCl_2$ (top) and $(MeCp)_2ZrCl_2/SiO_2$ (bottom). The line with visible noise component corresponds to the experimental data, while the smooth solid lines correspond to individual fitting lines and their sum.

coupling) are detected: one centered at 183.0 eV ($3d_{5/2}$), corresponding to ca. 57% of total area, and another one located at lower BE: 181.4 eV ($3d_{5/2}$).

Table 2 reports the zirconium BE for the different catalysts as neat complexes and supported on silica surface. In the homogeneous catalysts, higher alkyl donor ligands (*i*-Bu and *n*-Bu) induce a reduction in the Zr $3d_{5/2}$ BE as compared to the Me one (compare 181.7 or 181.6 eV versus 182.0 eV). This shift to lower BE corresponds to an increase of electronic density on the Zr atom due to contribution from the ligands. Considering both indenyl systems, the hydrogenation of the indenyl ring led also to a reduction

Table 2
Zr $3d_{5/2}$ lines BE extracted from fittings for homogeneous and silica-supported catalysts

Metallocene	BE (eV)	
	Neat complexes	Supported complexes
$(MeCp)_2ZrCl_2$	182.0	181.4 183.0
$(n\text{-BuCp})_2ZrCl_2$	181.6	182.4
$(i\text{-BuCp})_2ZrCl_2$	181.7	183.2
$Et(Ind)_2ZrCl_2$	182.4	180.4 182.6
$Et(IndH_4)_2ZrCl_2$	181.7	181.3 183.2

in the resulting BE in accordance with the expected resulting alkyl character.

After immobilization on silica surface, in the case of $(MeCp)_2ZrCl_2$, *rac*-Et$(Ind)_2ZrCl_2$ and *rac*-Et-$(IndH_4)_2ZrCl_2$ two surface species are observed: one with lower and another with higher BE in comparison to the line of the pure metallocene. The shift to higher BE indicates the presence of a more electron deficient species, and this can result from the exchange between chlorine atom and oxygen from silica, the latter being more electronegative. In the case of $(n\text{-}BuCp)_2ZrCl_2$ and $(i\text{-}BuCp)_2ZrCl_2$ only one species, having a higher BE in comparison to pure metallocene, was observed. This fact might be attributed to the presence of bulk ligands (*n*-Bu and *i*-Bu) that would hinder different types of complexation during the surface reaction. We cannot neglect the possibility that the lower BE species could be assigned to oxides decomposition moieties, generated during the surface reaction, since Zr $3d_{5/2}$ BE of ZrO_2 is 181.9 eV.

The homogeneous and supported metallocene catalysts were evaluated in ethylene/1-hexene copolymerization. The immobilization on silica surface lead to a reduction of the catalyst activity achieved by the homogeneous system (Fig. 2) because the silica surface plays the role of a huge ligand preventing the access of monomers to the catalysts center. Moreover, some of the zirconocene surface species might not be active, leading also to a reduction of the activity [24].

Comparing the three monosubstituted Cp catalysts, in the case of homogeneous polymerization, the order of their catalytic activities were: $(n\text{-}BuCp)_2ZrCl_2 > (MeCp)_2ZrCl_2 > (i\text{-}BuCp)_2ZrCl_2$. Monosubstituted cyclopentadienyl ring complexes ($(RCp)_2ZrCl_2$) have been studied previously [25,26], but it is generally difficult to compare results since reaction conditions are usually different. Electronic and steric effects associated with R substituents can influence on the activity and polymer properties. Electron donating groups enhance the activity, while steric hindrance can affect the polymerization kinetics [27]. The electronic effects of the substituents can be evaluated by the metal core-level binding energies as showed in Table 2. Considering the homogenous systems, and taking into account the pass energy 11.75 eV with 0.05 eV resolution, an increase in the Zr 3d BE in the following order is observed: $(n\text{-}BuCp)_2ZrCl_2 < (i\text{-}BuCp)_2ZrCl_2 < (MeCp)_2ZrCl_2$. Electronic effects seems to dominate when comparing the higher reactivity of *n*-Bu to that exhibited by Me substituent. The lower catalytic activity of $(i\text{-}BuCp)_2ZrCl_2$ cannot be explained on the grounds of electronic effects because this catalyst has almost the same electronic donating ability as $(n\text{-}BuCp)_2ZrCl_2$. Therefore, the lower catalyst activity shown by $(i\text{-}BuCp)_2ZrCl_2$ might be due to higher steric hindrance from such ligand.

Catalytic activities in the supported system followed the same trend as in the case of homogeneous

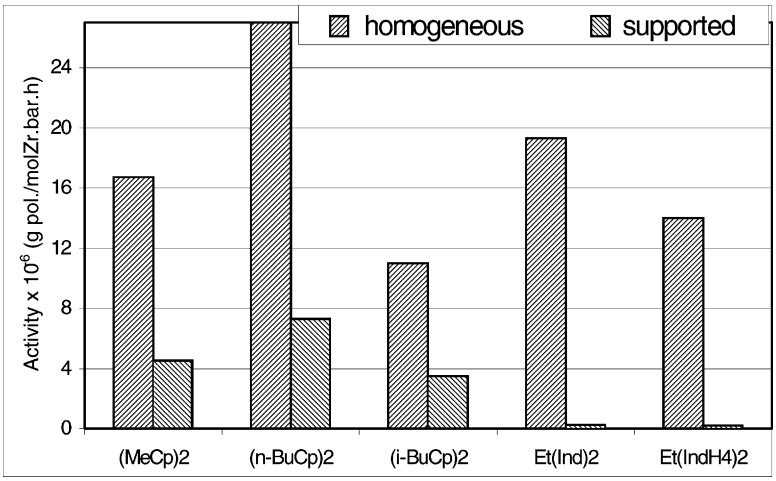

Fig. 2. Catalyst activity of homogeneous and supported systems in ethylene/1-hexene copolymerization. Reaction conditions: $[Zr] = 2 \times 10^{-6}$ mol; [1-hexene] = 0.38 M; [Al]/[Zr] = 2500; pressure = 1.6 bar; reaction time = 30 min.

Table 3
Characterization of copolymers obtained using homogeneous and supported systems

Catalyst	[H] (mol%)[a]	T_m (°C)[b]	X_c (%)[c]	M_w (g/mol)	M_w/M_n
$(MeCp)_2ZrCl_2$	3.3	112.8	25	126000	2.8
$(n\text{-}BuCp)_2ZrCl_2$	4.5	104.5	29	47200	2.5
$(i\text{-}BuCp)_2ZrCl_2$	3.0	112.8	29	68300	2.5
$Et(Ind)_2ZrCl_2$	6.7	88.3	7	68000	2.4
$Et(IndH_4)_2ZrCl_2$	7.3	81.8	6	64200	2.6
$(MeCp)_2ZrCl_2/SiO_2$	3.0	113.1	28	134000	2.4
$(n\text{-}BuCp)_2ZrCl_2/SiO_2$	3.6	108.8	30	130000	2.2
$(i\text{-}BuCp)_2ZrCl_2/SiO_2$	2.3	121.7	21	187000	2.5
$Et(Ind)_2ZrCl_2/SiO_2$	1.5	117.0	47	245000	1.8
$Et(IndH_4)_2ZrCl_2/SiO_2$	2.5	113.8	21	289000	1.6

Ethylene in solution = 0.11 M; 1-hexene in solution = 0.38 M.
[a] [H]: [1-hexene].
[b] T_m: melting temperature
[c] X_c: crystalinity.

ones. Considering the Cp substituted supported catalysts and the highest BE (in the case of catalysts possessing two surface species), $(n\text{-}BuCp)_2ZrCl_2$ was also the most active catalyst and the one with the highest electron-donating ability of the ligand. The lowest catalytic activity in the case of $(i\text{-}BuCp)_2ZrCl_2$ may be due to its higher electron deficient metal center and to its higher steric effect. A similar relation between lower BE and higher catalyst activity was already reported in the literature [12,28].

The homogeneous *ansa*-metallocenes were very active *rac*-$Et(IndH_4)_2ZrCl_2$ being less active than *rac*-$EtInd_2ZrCl_2$. On the other hand, the supported *ansa*-metallocenes systems were not very active probably due to steric hindrance on the metallic center caused by silica.

Copolymers characterization is shown in Table 3. The *ansa*-metallocenes produced copolymers with the highest comonomer incorporation in the homogeneous system but yield copolymers with the lowest incorporation in the supported systems. These results suggest the high steric hindrance caused by the presence of the bridge allied with the silica grain surface in the active center of the supported system.

Comparing the monosubstituted Cp catalysts, 1-hexene incorporation scales with the catalytic activity for both homogeneous and supported systems. Melting temperatures and crystallinities agree with 1-hexene incorporations, especially in the case of homogeneous systems, the highest degree of incorporated copolymer leads to the lowest melting temperature and crystallinity, as expected. Supported catalysts produced copolymers with higher molecular weights than the homogeneous ones. This fact was already noted [27] and it has been attributed to the formation of a more stabilized structure on the surface due to steric interaction, preventing deactivation by bimolecular processes [22]. In the case of supported systems, less active catalysts produce polymers with higher molecular weights probably due to low propagation and termination rate ratios. Supported systems produced copolymers with narrow molecular weight distribution, which indicates the homogeneity of active sites. It seems that not all the different generated surface species might be active, as already suggested in the literature [24].

4. Conclusions

Homogeneous and supported metallocene catalysts with different ligands have been evaluated in terms of resulting metal loading on silica, of different electron donation and steric hindrance effects to the Zr metal center and of ethylene/1-hexene copolymerization activity. Silica grafted with $(n\text{-}BuCp)_2ZrCl_2$, $(i\text{-}BuCp)_2ZrCl_2$ and *rac*-$Et(IndH_4)_2ZrCl_2$ presented the lowest metal contents among the studied metallocenes. Binding energies determined by XPS indicated the generation of more electron deficient species

when metallocene is grafted on silica, which can be attributed to the formation of a bond between metal and oxygen from silica.

Catalyst activities in ethylene/1-hexene copolymerization were dependent on electronic effects when *n*-Bu and Me monosubstituted Cp were compared and on steric effects when comparing *n*-Bu to *i*-Bu groups. High activities observed in the case of homogeneous *rac*-Et(Ind)$_2$ZrCl$_2$ catalyst system might be attributed to the presence of the bridge that promote the olefin insertion. In such system electronic effects does not seem to predominate. The very low activities presented by *ansa*-metallocenes in the supported catalyst were attributed to the steric hindrance caused by the silica surface. (*n*-BuCp)$_2$ZrCl$_2$ was the catalyst which presented better catalytic activities in both, homogeneous and supported systems, besides the highest comonomer incorporation among the supported ones.

Acknowledgements

We thank PADCT/CNPq/Brazil, CNPq, FAPERGS and OPP Petroquímica S.A for financial support and Witco for MAO donation. Financial support for Prof. J.H.Z. dos Santos has been provided by the Japan Society for Promotion of Science (JSPS).

References

[1] Global Plastics and Polymers Market Report, CMAI, Houston, 10 January 1999.
[2] W. Kaminsky, Macromol. Chem. Phys. 197 (1996) 3907.
[3] (a) G.G. Hlatky, Chem. Rev. 100 (2000) 1347;
(b) H.T. Ban, T. Arai, C.-H. Ahn, T. Uozumi, K. Soga, Curr. Trends Polym. Sci. 4 (1999) 47;
(c) M.R. Ribeiro, A. Deffieux, M.F. Portela, Ind. Eng. Chem. Res. 36 (1997) 1224.
[4] R.J.L. Graff, B. Kortleve, C.G. Vonk, Polym. Lett. 8 (1970) 735.
[5] (a) J.H.Z. dos Santos, S. Dorneles, F.C. Stedile, J. Dupont, M.C. Forte, I.J.R. Baumvol, Macromol. Chem. Phys. 198 (1997) 3529;
(b) J.H.Z. dos Santos, A. Larentis, M.B. da Rosa, C. Krug, I.J.R. Baumvol, J. Dupont, F.C. Stedile, M.C. Forte, Macromol. Chem. Phys. 200 (1999) 751.
[6] D. Lee, S. Shin, D. Lee, Macromol. Symp. 97 (1995) 195.
[7] D. Lee, K. Yoon, S. Noh, Macromol. Rapid Commun. 18 (1997) 427.
[8] (a) K. Soga, T. Shiono, H.J. Kim, Macromol. Chem. Phys. 194 (1993) 3499;
(b) B.L. Moroz, N.V. Semikolenova, A.V. Nosov, V.A. Zakharov, S. Nagy, N.J. O'Reilly, J. Mol. Catal. A: Chem. 130 (1998) 121;
(c) J.H.Z. dos Santos, P.P. Greco, F.C. Stedile, J. Dupont, J. Mol. Catal. A: Chem. 154 (2000) 103.
[9] K. Soga, H.J. Kim, T. Shiono, Macromol. Chem. Phys. 195 (1994) 3347.
[10] S.C. Hong, H.T. Ban, N. Kishi, J. Jin, T. Uozumi, K. Soga, Macromol. Chem. Phys. 199 (1998) 1393.
[11] M. Stork, M. Koch, M. Klapper, K. Mullen, H. Gregorius, U. Rief, Macromol. Rapid Commun. 20 (1999) 210.
[12] J.H.Z. dos Santos, H.T. Ban, T. Teranishi, T. Uozumi, T. Sano, K. Soga, J. Mol. Catal. A: Chem. 158 (2000) 559.
[13] G.B. Galland, M. Seferin, R.S. Mauler, J.H.Z. dos Santos, Polym. Int. 48 (1990) 660.
[14] F.C. Stedile, J.H.Z. Dos Santos, Nucl. Instrum. Meth. B 136-139 (1998) 1259.
[15] F.C. Stedile, J.H.Z. Dos Santos, Phys. Stat. Sol. 173 (1999) 123.
[16] J.C. Randall, Macromol. Chem. Phys. C29 (1989) 201.
[17] D.D. Traficante, L.R. Steward, Concepts Magn. Resonance 6 (1994) 131.
[18] E.F. Vansant, P. van der Voort, K.C. Vrancken, Stud. Surf. Sci. Catal. 93 (1995) 3.
[19] J.H.Z. dos Santos, C. Krug, M.B. da Rosa, F.C. Stedile, J. Dupont, M.C. Forte, J. Mol. Catal. A: Chem. 139 (1999) 199.
[20] M.C. Sacchi, D. Zucchi, I. Tritto, P. Locatelli, Macromol. Rapid Commun. 16 (1995) 581.
[21] J. Tait, R. Ediati, in: Proceedings of MetCon'97, Houston, USA, 4–5 June 1997.
[22] W. Kaminsky, F. Renner, Macromol. Rapid Commun. 14 (1993) 239.
[23] S. Collins, W.M. Kelly, D.A. Holden, Macromolecules 25 (1992) 1780.
[24] A. Muñoz-Escalona, L. Méndez, J. Sancho, P. Lafuente, B. Peña, W. Michiels, G. Hidalgo, M.F. Martinez-Nuñez, in: W. Kaminsky (Ed.), Metalorganic Catalysts for Synthesis and Polymerization, Springer, Heidelberg, Vol. 38, 1999.
[25] J.C.W. Chien, B.P. Wang, J. Polym. Sci. Part A: Polym. Chem. 28 (1990) 15.
[26] J. A Ewen, Stud. Surf. Sci. Catal. 25 (1986) 271.
[27] P.C. Möhring, N.J. Coville, J. Organomet. Chem. 479 (1994) 1.
[28] M.C. Haag, C. Krug, J. Dupont, G.B. Galland, J.H.Z. dos Santos, T. Uozumi, T. Sano, K. Soga, J. Mol. Catal. A: Chem. 169 (2001) 275.